

NINETEENTH EUROPEAN ROTORCRAFT FORUM

Paper n° H9

**TRIM, STABILITY, AND FREQUENCY RESPONSE SIMULATION  
OF AN ARTICULATED ROTOR HELICOPTER IN TURNING FLIGHT**

by

Roberto Celi

Center for Rotorcraft Education and Research  
Department of Aerospace Engineering  
University of Maryland, College Park, MD 20742, USA

Frederick D. Kim

NASA Ames Research Center  
Moffett Field, California, USA.

September 14-16, 1993  
CERNOBBIO (Como)  
ITALY

ASSOCIAZIONE INDUSTRIE AEROSPAZIALI  
ASSOCIAZIONE ITALIANA DI AERONAUTICA ED ASTRONAUTICA



# TRIM, STABILITY, AND FREQUENCY RESPONSE SIMULATION OF AN ARTICULATED ROTOR HELICOPTER IN TURNING FLIGHT

Roberto Celi<sup>1</sup>

Frederick D. Kim<sup>2</sup>

**Abstract** — This paper describes the results of a study focusing on the behavior of an articulated rotor helicopter in steady coordinated turns. The model includes fuselage, inflow, propulsion system, and individual blade flap and lag dynamics. Results for trim states, poles, and on- and off-axis frequency responses are presented. Comparisons with trim flight test data indicate good correlation for most trim variables over a wide ranges of bank angles. Stability results indicate that the phugoid is slightly destabilized by a right turn and is stabilized by a left turn, although in both cases it remains unstable. The Dutch roll mode tends to be destabilized by turns in both directions and couples with the rotor speed mode in right-handed turns, which also slightly decrease the damping of the short period mode. A substantial decrease of the damping of the regressive lag mode is also observed. An increase in cross-couplings is evidenced by an increase in the magnitude of the off-axis response across a wide frequency band.

## 1. Introduction

Operational requirements for military helicopters place great importance on turning flight conditions, because these helicopters may spend extended periods of time in nap-of-the-earth flight where the ability to quickly and safely avoid obstacles is vital. Good maneuverability and agility characteristics are also required to escape enemy fire and for air-to-air combat. Although the maneuver requirements for civil helicopters are not equally stringent, some of the situations in which these helicopters must maneuver are especially critical, for example, take-off and landing, and evasive actions to avoid ground obstacles or other aircraft. A fairly modest amount of research on the dynamics of helicopters in maneuvering flight has been reported in the literature.

One of the earlier studies on the subject is due to Chen [1], who derived a mathematical model applicable to turning flight conditions, and used it to examine the flight dynamics of several rotorcraft configurations in steep left and right high- $g$  turns. One of the conclusions of this study was that the coupling of the lateral and longitudinal motion becomes more severe in high- $g$  turns, especially at lower speeds. The direction of the turn also affects the dynamic characteristics. For example, a right handed turn tends to stabilize the spiral mode and destabilize the phugoid, whereas a left turn tends to do the opposite. Another interesting conclusion of this study is that the performance of a flight control system designed based exclusively on straight flight dynamics can be degraded severely when the helicopter enters a turn. A study that focused on the short period longitudinal dynamics during maneuvers was carried out by Houston [2]. The study was conducted using a

---

<sup>1</sup>Associate Professor, Center for Rotorcraft Education and Research, Department of Aerospace Engineering, University of Maryland, College Park, USA.

<sup>2</sup>Aerospace Engineer, NASA Ames Research Center, Moffett Field, California, USA.

linearized six degree of freedom mathematical model of the SA-330 Puma helicopter. Stability derivatives of the Puma in left and right turns with bank angles of up to 60 degrees at airspeeds of 60 and 100 knots were calculated. One of the major conclusions of this study was that the traditional short period approximation is inadequate for predicting stability and control characteristics in high bank angle turns. The approximation fails because strong cross couplings arise in these flight conditions, and their magnitude increases with bank angle. Houston concluded that the variations in the stability derivatives come from all sources, aerodynamic, inertial, kinematic, and gravitational, with the rotor playing a fundamental role.

A mathematical model describing trim conditions in coordinated, steady, helical turns, first formulated by Chen [3, 4], was extended by Celi to take into account the steady-state periodic motion of flexible main rotor blades [5], and coupled with an aeroelastic stability and response analysis to study the aeroelastic characteristics of an isolated hingeless rotor helicopter in turning flight. This study was further extended by Spence [6] to include the dynamic coupling between rotor and fuselage. These studies indicate that the maneuvering envelope of hingeless rotor helicopters may be limited by aeroelastic stability considerations. The rotor modes that may suffer substantial degradations of stability are the second lag mode in level turns, and the first lag mode in descending turns.

The objective of this paper is to present a series of results concerning the dynamics of an articulated rotor helicopter in steady, coordinated, level turns. The results are obtained using a blade element type nonreal time simulation model, and consist of trim states, poles, and frequency response plots for various flight speeds and turn rates.

## 2. Mathematical Model

The mathematical model of the helicopter is described in detail in Refs. [7, 8], and only a brief outline will be presented here. The model, which is an extension of the Genhel model originally formulated by Howlett [10], consists of a nonlinear, blade element type representation of a single rotor helicopter with a rigid fuselage. No small angle assumptions are invoked for the angles of attack of rotor and fuselage. Therefore the model is valid for a wide range of fuselage attitudes. The main rotor blades are individually modeled as rigid bodies undergoing flap and lag motion. An empirical correction for the dynamic twist due to the torsional dynamics of the blades is also included. A three state [9] and a one state dynamic inflow models are used for the main rotor and the tail rotor respectively. Aerodynamic forces are calculated using blade element theory with table look-up for lift and drag coefficients. The aerodynamics of the fuselage and the empennage is modeled using tables of aerodynamic coefficients obtained from wind tunnel tests. The equations of motion of the fuselage are formulated and solved in a fixed system of body axes. The equations of motion of the rotor are formulated and solved in a rotating coordinate system. A rotating-to-fixed coordinate transformation is carried out for the rotor variables, therefore the entire output of the computer program implementing the model is in the body fixed coordinate system. The mathematical model used for the propulsion system is based on that derived by Ballin [11]. Thus

the states included in the model are the main rotor speed  $\Omega$ , the rotational speed  $N_G$  of the gas generator, the compressor discharge pressure  $p_3$ , the gas generator inlet pressure  $p_{41}$ , and the power turbine inlet pressure  $p_{45}$ .

A linearized set of small perturbation equations of motion can be extracted from the nonlinear model. The coefficients of the model are obtained numerically, using finite difference approximations. The order of the system is 32. Additionally, the dynamics of each of the four pitch control actuators can be represented by a second order transfer function. Therefore, another 8 states can be appended to the linearized model, for a total overall size of 40 states.

The calculation of the trim state of the helicopter consists of the simultaneous solution of two coupled sets of nonlinear algebraic equations. The first set includes certain kinematic relations that must be satisfied in a turn, as well as the rigid body Euler dynamic equations with linear and angular accelerations set to zero, and  $\dot{\theta} = \dot{\phi} = 0$ . A straight flight condition is treated as a special type of turn with  $\dot{\psi} = 0$ . The second set of equations describes the steady state behavior of the rotor, and is obtained by transforming the ordinary differential equations of motion of the blade into a set of nonlinear algebraic equations using a global Galerkin method. The solution of the fuselage trim problem, described by the first set of equations, is coupled with the solution of the blade response problem, described by the second set of equations, because the forces and moments generated by the rotor depend on the equilibrium position of the blades. For a given flight condition, defined by forward speed  $V$ , flight path angle  $\gamma$ , and turn rate  $\dot{\psi}$ , the solution of the trim problem yields the steady state values of main rotor and tail rotor pitch controls, angle of attack  $\alpha$  and sideslip  $\beta$  of the fuselage, average inflow over the main and the tail rotor disks, fuselage pitch and roll attitude angles  $\theta$  and  $\phi$ , and roll, pitch, and yaw rates  $p$ ,  $q$ , and  $r$ . The trim solution also provides the steady state periodic motion of the blades in flap, and lag in the form of a truncated Fourier series. These quantities define the equilibrium position of the helicopter.

The procedure followed to "trim" the engine was not presented in Ref. [7] and will now be described here. Such a procedure is needed to accommodate the particular formulation of the engine equations of motion. The aircraft and rotor trim procedure described above is carried out independently of the propulsion system and, when completed, yields the total engine power requirements which become the starting point of the engine trim procedure. The torque produced by the engine is dependent on the fuel flow  $W_f$ , the gas generator speed  $N_G$ , and the thermodynamic states  $p_3$ ,  $p_{41}$ , and  $p_{45}$ . An interpolation table, specific to the General Electric T700 engine, provides these values as a function of a torque estimate factor  $Q'$  [11]. For each value of  $Q'$  the interpolation table provides one set of values of the fuel flow and of the engine states. However, depending on the flight conditions, the actual torque corresponding to this set will usually be different from the required torque. Therefore the torque estimate factor  $Q'$  is adjusted iteratively until the actual torque produced by this combination of fuel flow and engine states matches the torque required by the aircraft. When this occurs, the rotor on average will neither accelerate nor decelerate. In other words it will be:

$$\int_0^{2\pi} \dot{\Omega} d\psi = 0$$

This is rigorously only a preliminary solution, because only the requirement on the rotor speed has

been enforced. At this point the gas generator speed  $N_G$  and the thermodynamic states  $p_3, p_{41}$ , and  $p_{45}$  may not have reached a steady-state value. If necessary, this preliminary equilibrium solution may be further refined by using these values of the states as initial conditions for the engine equations, integrating the engine equations until a true steady state is reached, and adjusting the initial conditions if the torque obtained at the end of this process has deviated too much from the required value [8].

#### 4. Results

The trim procedure was validated by comparing the computed trim solutions with the flight test results of Ref. [12]. The flight test was conducted with the UH-60 flying at 5250 feet with a gross weight of 16000 lbs, corresponding to a  $C_T/\sigma = 0.080$ . The stabilator angle of attack was adjusted with airspeed, and this variation was taken into account in the present validation. The engine degrees of freedom were deactivated because the mathematical model of the engine, in the present study, is calibrated for the aircraft flying at sea level. Trim solutions are obtained for increasing values of the turn rate  $\bar{\psi}$ , but are plotted in the figures as a function of the bank angle  $\phi$  to maintain consistency with Ref. [12]. It should be pointed out that for a fixed wing aircraft the relationship between the bank angle  $\phi$  and the turn rate  $\bar{\psi}$  is simply  $\tan \phi = \bar{\psi}V/g$  [13, pp. 423-425], whereas for a helicopter the relationship is given by [3]:

$$\sin \phi = \frac{\bar{\psi}V}{g}(\cos \alpha \cos \phi + \sin \alpha \tan \theta) \cos \beta$$

therefore it is not possible to determine directly which value of the turn rate corresponds to a given value of the bank angle, and the complete trim problem needs to be solved. Figures 1 and 2 compare the predicted trim results and the flight test data at flight speeds of 60 kts and 100 kts respectively, corresponding to advance ratio of  $\mu = 0.13$  and  $\mu = 0.22$ . At 60 kts the main rotor power is slightly overpredicted. The collective pitch is also slightly overpredicted, which may imply that the model predicts a slightly higher induced power than actually required. The pitch attitude is predicted within less than one degree for left-handed turns, but it is overpredicted, i.e. more "nose-up" for right-handed turns. In this case the flight tests indicate that the pitch attitude does not change substantially with turn rate; if this trend is correct, it is not captured by the model. Pitch rate, longitudinal cyclic, lateral cyclic and yaw rates are all in good agreement with the flight test results. Some discrepancies are instead observed for the trim values of pedal, but these may be partially due to some uncertainties in the details of the pedal rigging characteristics [12]. At 100 kts the model overpredicts substantially the power required in tight turns, possibly because the stall model is limited to static stall and may not be truly representative of these tight turn conditions. The required collective pitch is overpredicted at high bank angles as well. The correlation is fair for the pitch attitude, and again good for all the remaining quantities plotted in the figure. The pedal trim values again show some discrepancies, and is now underpredicted.

Table 1 shows the poles of the helicopter flying at 80 kts in the following three conditions: straight flight, 2-g right-handed turn, and 2-g left-handed turn. The main character of each mode

is listed in the Table. It should be kept in mind, however, that all the modes are coupled to some extent, especially in turning flight conditions. Compared with straight flight conditions, the phugoid is slightly destabilized by a right turn and is somewhat stabilized by a left turn, although in both cases it remains unstable. The same trend was observed in Ref. [1] for a simulated hingeless rotor configuration. The Dutch roll mode tends to be destabilized by turns in both directions. In a right turn one pole of the complex conjugate pair becomes real and positive, while the other joins the rotor speed degree of freedom to generate a stable complex conjugate pair. This behavior is rather different from that observed in Ref. [1], in which turns did not have a significant influence on the Dutch roll mode. The short period longitudinal mode of the SA-330 Puma helicopter was examined in detail in Ref. [2]. The results show a movement of the short period pole of the Puma from ( $\zeta = 0.53, \omega = 1.82$ ) in straight flight at 60 knots to ( $\zeta = 0.57, \omega = 1.85$ ) in a turn with bank angle  $\phi = 45$  degrees at 60 knots. This implies a slight stabilizing effect for a positive bank angle, corresponding to a positive turn rate. The results shown in Table 1 indicate the opposite effect for the UH-60, in which a right-handed turn slightly decreases the damping of the short period mode. The difference is probably simply due to the fact that the main rotors of the two aircraft turn in opposite directions. The main effect of 2-g turns on the rotor degrees of freedom is a substantial decrease of the damping of the regressive lag mode, which however remains well damped.

The effect of turning flight conditions on the frequency response of the helicopter is shown in Figures 3 and 4, for the on-axis and off-axis response to pilot inputs respectively. It was not possible to validate the frequency responses predicted by the mathematical model for turning flight conditions because no experimental data are currently available. A frequency domain validation of the present model for the case of straight forward flight can be found in Ref. [7]. The results presented in Figures 3 and 4 refer to a flight speed of 80 kts, and show curves for straight flight, a 2-g right-handed turn and a 2-g left-handed turn.

The effects on the on-axis response can be divided into two categories, namely those on the aircraft dynamics, that appear at frequencies below 1-2 rad/sec, and those on the rotor, that appear at the frequency of the regressive lag mode, around 18-20 rad/sec, and higher. In the frequency band between 2 and 10-15 rad/sec, the effects of the turn on the on-axis response appear to be small. The effects related to rotor dynamics manifest themselves especially in the pitch and roll on-axis response, since these degrees of freedom couple with the regressive lag mode, and are negligible in the heave and yaw response. At lower frequencies the amplitude of the roll response decreases in a turn, whereas that of the pitch response tends to increase slightly. Substantial phase changes can be observed in both cases, with the delay increasing in left handed turns, and increasing in right handed turns.

Figure 4 shows the frequency response in pitch rate  $q$  due to lateral cyclic, and in roll rate  $p$  due to longitudinal cyclic. For this pair of off-axis responses, the effects of turns appear throughout the frequency range, and clearly show an increase in the magnitude of the off-axis response, and therefore of the dynamic couplings, in turning flight conditions. A substantial increase in phase is especially evident in the  $q/\delta_{lat}$  response at frequencies above 3-4 rad/sec, for the case of left turns. This effect may be destabilizing in high-gain piloting situations or if the helicopter is equipped with

high-gain flight control systems designed based on the straight flight dynamic characteristics.

## 5. Summary and Conclusions

The results of a study focusing on the behavior of an articulated rotor helicopter in steady coordinated turns have been presented. The results have been obtained using a blade element type, nonreal-time simulation model that includes fuselage, inflow, propulsion system, and individual blade flap and lag dynamics. The model can be used to calculate trim states, extract high-order linearized models, and free flight response to arbitrary pilot inputs. Lack of experimental data precluded a thorough validation of the model, but comparisons with trim flight test data indicate good correlation for most trim variables over a wide ranges of bank angles. Stability results indicate that, compared with straight flight conditions, the phugoid is slightly destabilized by a right turn and is somewhat stabilized by a left turn, although in both cases it remains unstable. The Dutch roll mode tends to be destabilized by turns in both directions and couples with the rotor speed mode in right-handed turns, which also slightly decrease the damping of the short period mode. A substantial decrease of the damping of the regressive lag mode is also observed, but the mode remains well damped. Finally, an increase in cross-couplings is evidenced by an increase in the magnitude of the off-axis response across a wide frequency band.

## References

- [1] Chen, R. T. N., "Flight Dynamics of Rotorcraft in Steep High-g Turns," *Journal of Aircraft*, Vol. 21, No. 1, Jan. 1984.
- [2] Houston, S.S., "On the Analysis of Helicopter Flight Dynamics During Maneuvers," *Proceedings of the Eleventh European Rotorcraft Forum*, London, England, Sept. 1985.
- [3] Chen, R. T. N., and Jeske, J. A., "Kinematic Properties of the Helicopter in Coordinated Turns," NASA Technical Papers 1773, Apr. 1981.
- [4] Chen, R. T. N., and Jeske, J. A., "Influence of Sideslip on the Helicopter in Steady Coordinated Turns," *Journal of the American Helicopter Society*, Vol. 27, (4), Oct. 1982.
- [5] Celi, R., "Hingeless Rotor Dynamics in Coordinated Turns," *Journal of the American Helicopter Society*, Vol. 36, (4), Oct. 1991.
- [6] Spence, A., and Celi, R., "Coupled Rotor-Fuselage Dynamics in Turning Flight," *Proceedings of the AIAA Dynamics Specialist Conference*, Dallas, Texas, April 1992, pp. 292-301.
- [7] Kim, F.D., Celi, R., and Tischler, M.B., "Forward Flight Trim and Frequency Response Validation of a Helicopter Simulation Model," *Proceedings of the 47th Annual Forum of the American Helicopter Society*, Phoenix, Arizona, May 1991, pp. 155-168, to appear in the *Journal of Aircraft*.



- [8] Kim, F. D., "Formulation and Validation of High-Order Mathematical Models of Helicopter Flight Dynamics," Ph.D. Dissertation, Department of Aerospace Engineering, University of Maryland, College Park, September 1991.
- [9] Pitt, D.M., and Peters, D.A., "Theoretical Prediction of Dynamic Inflow Derivatives," *Vertica*, Vol. 5, No. 1981, pp. 21-34.
- [10] Howlett, J.J., "UH-60A Black Hawk Engineering Simulation Program—Volume II—Mathematical Model," NASA CR-166309, Dec. 1981.
- [11] Ballin, M. G., "A High Fidelity Real-Time Simulation of a Small Turboshaft Engine," NASA TM-100991, July 1988.
- [12] Abbott, W. Y., Benson, J. O., Oliver, R. G., and Williams, R. A., "Validation Flight Tests of UH-60A for Rotorcraft Systems Integration Simulator (RSIS)," Report No. USAAEFA-79-24, U. S. Army Aviation Engineering Flight Activity, July 1982.
- [13] Etkin, B., *Dynamics of Flight—Stability and Control*, John Wiley and Sons, 1982.

| Mode               | Straight         | 2-g Right Turn   | 2-g Left Turn    |
|--------------------|------------------|------------------|------------------|
| p41                | (4162.1)         | (3735.8)         | (4738.2)         |
| p45                | (4597.2)         | (4725.3)         | (3695.8)         |
| p3                 | (51.672)         | (53.387)         | (53.299)         |
| Gas Generator      | (1.8863)         | (2.5757)         | (2.5852)         |
| Dynamic Twist      | [0.2853,172.28]  | [0.2853,171.57]  | [0.2854,172.32]  |
| Progressive Flap   | [0.2293,51.763]  | [0.2273,51.636]  | [0.2303,51.885]  |
| Progressive Lag    | [0.1266,36.756]  | [0.0781,37.788]  | [0.0806,37.957]  |
| Collective Lag/RPM | (45.949)         | (26.927)         | (27.477)         |
|                    | (39.268)         | (11.398)         | (11.928)         |
| Reactionless Flap  | [0.4638,28.039]  | [0.4451,27.766]  | [0.4526,28.084]  |
| Collective Flap    | [0.3251,26.755]  | [0.3258,26.585]  | [0.3249,26.898]  |
| Regressive Lag     | [0.1887,18.483]  | [0.1258,18.218]  | [0.1338,18.190]  |
| Reactionless Lag   | [0.7127,8.3950]  | [0.3749,8.5016]  | [0.3350,8.8211]  |
| Collective Lag     | (5.8766)         | (13.624)         | (15.074)         |
| Regressive Flap    | [0.8767,3.6697]  | [0.8262,4.4350]  | [0.8332,4.2175]  |
| Tail Rotor Inflow  | (64.430)         | (67.720)         | (69.710)         |
| Main Rotor Inflow  | (27.901)         | (37.926)         | (38.389)         |
| Inflow Harmonics   | [0.9323,14.334]  | [0.8412,16.573]  | [0.8729,16.136]  |
| Delayed Downwash   | (8.1559)         | (8.1199)         | (8.1304)         |
| Delayed Sidewash   | (8.0843)         | (8.0622)         | (8.0708)         |
| Sprial             | (1.4968)         | [0.8427,1.6086]  | [0.9089,1.5036]  |
|                    | (1.3237)         |                  |                  |
| Short Period       | [0.3623,1.3552]  | [0.3478,1.5078]  | [0.3642,1.5193]  |
| RPM/Dutch Roll     | (0.3207)         | (0.2532)         | [0.7432,0.4022]  |
| Yaw                | (0.0000)         | (0.0000)         | (0.0000)         |
| Dutch Roll         | [-0.1100,0.0654] | [-0.1623,0.5464] | (-0.2768)        |
| Phugoid            | [-0.5147,0.4615] | [-0.5259,0.3954] | [-0.4679,0.6480] |

Table 1: Poles of the helicopter in straight flight, and right 2-g and left 2-g turns. Shorthand notation:  $[\zeta; \omega]$  implies  $[s^2 + 2\zeta\omega s + \omega^2]$ , and (a) implies  $(s + a)$ .

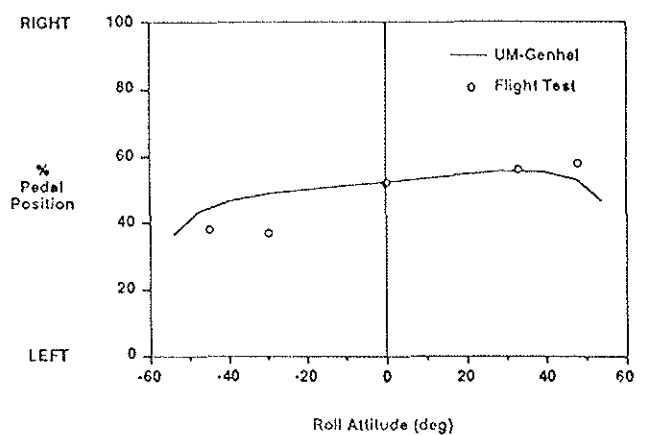
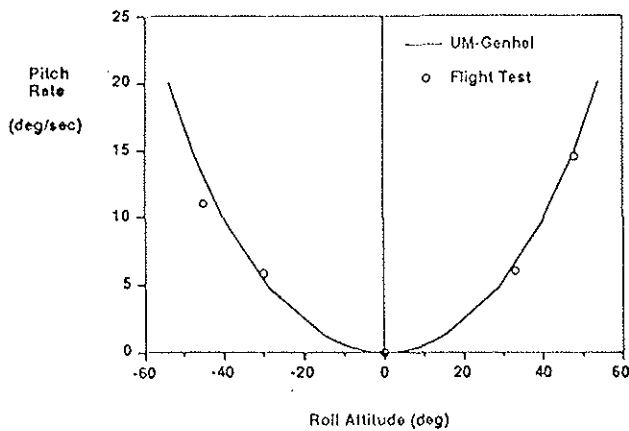
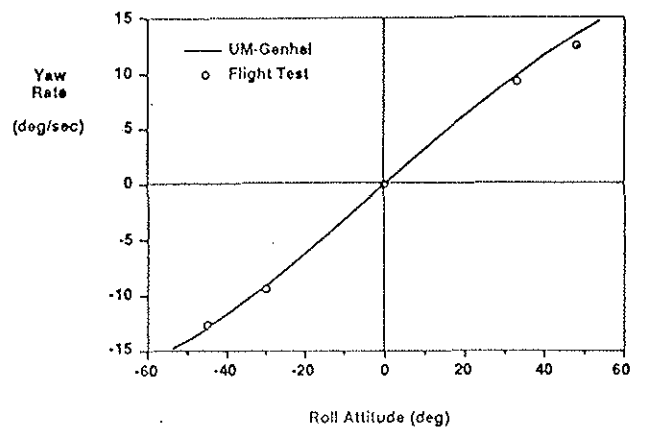
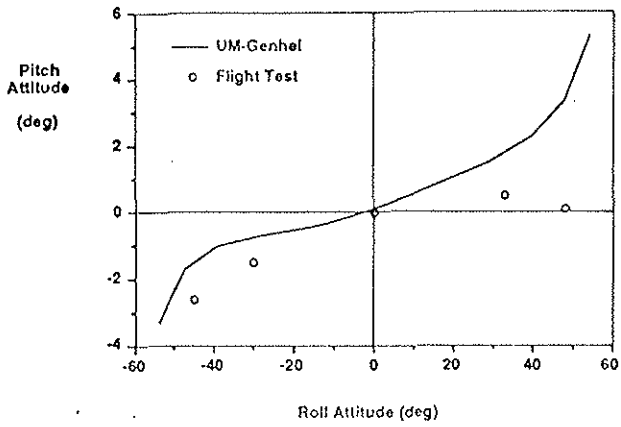
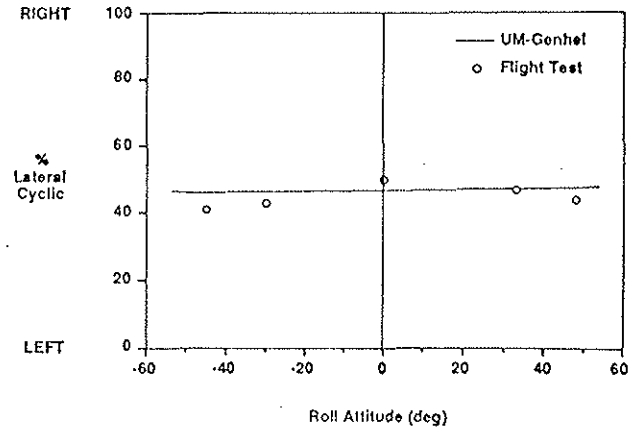
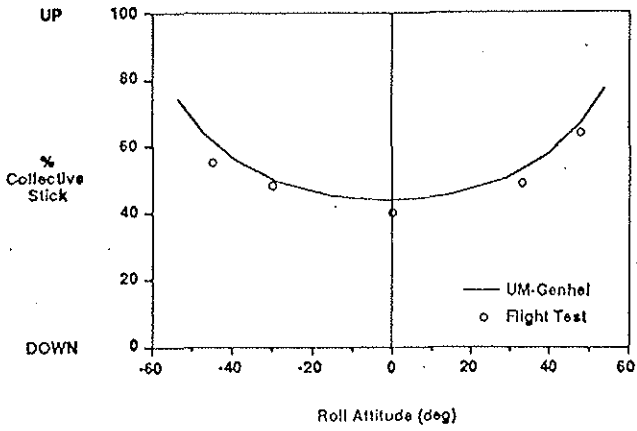
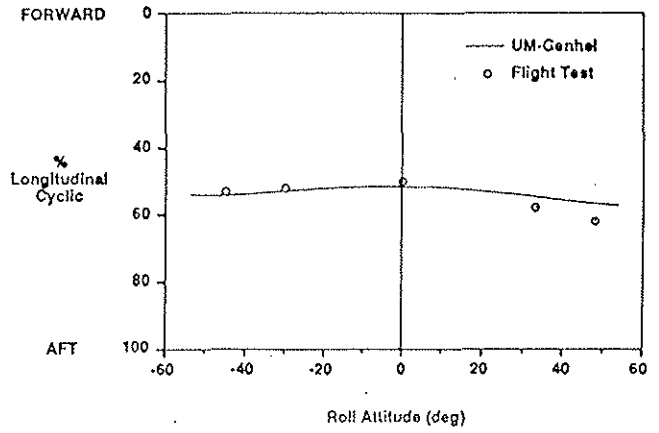
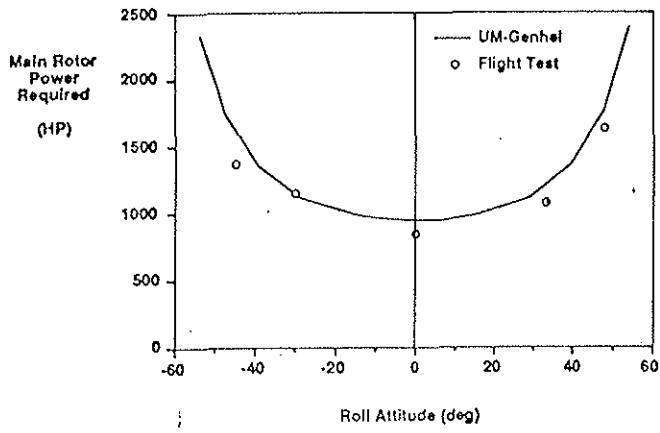


Figure 1: Trim state in coordinated steady level turn; V=60 kts.

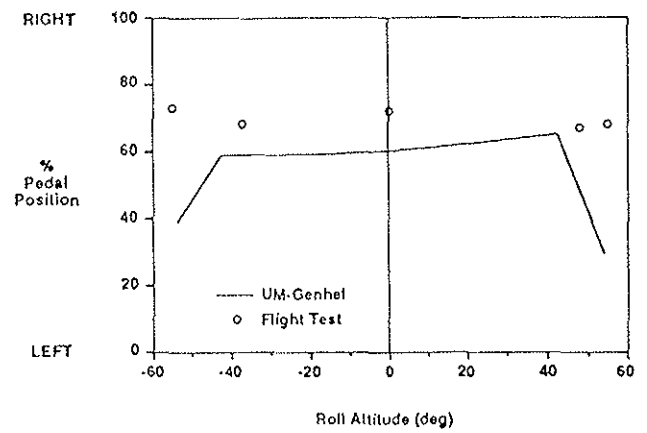
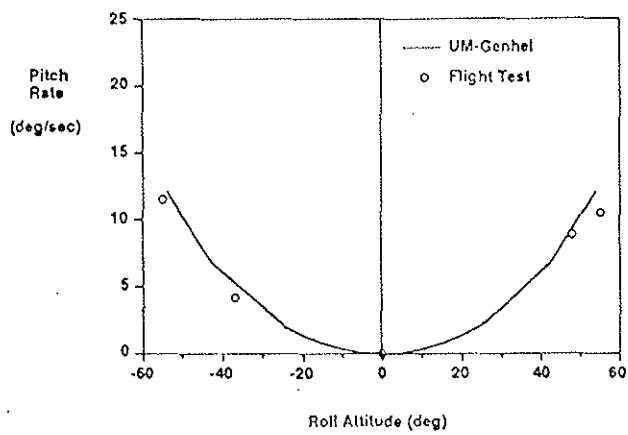
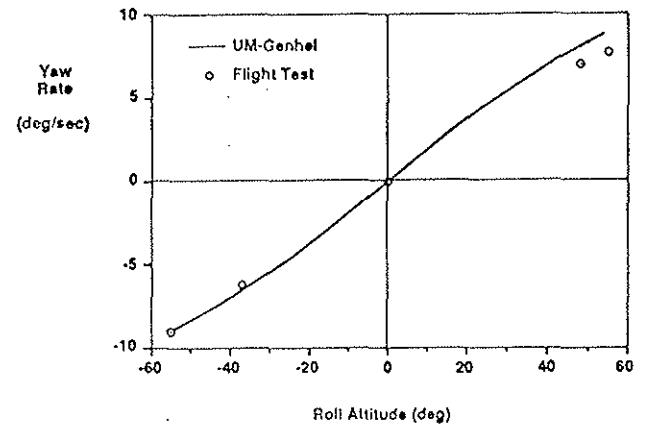
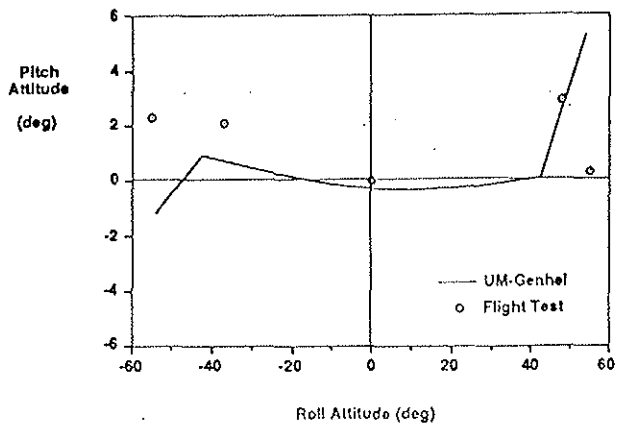
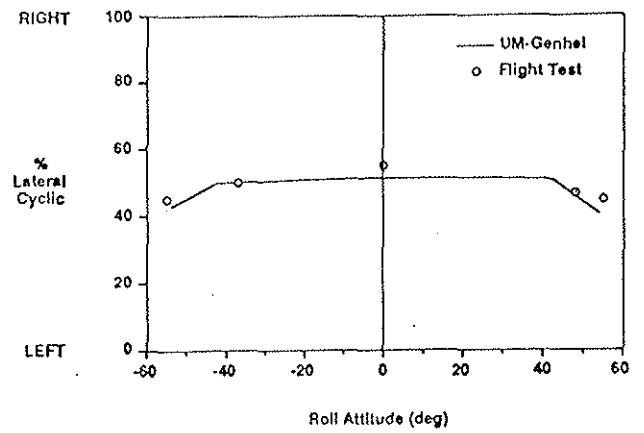
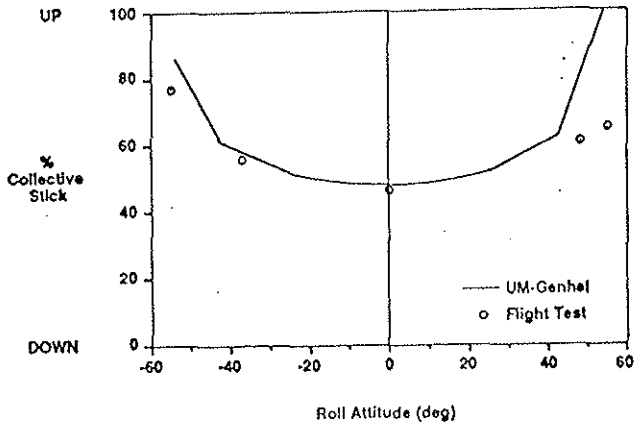
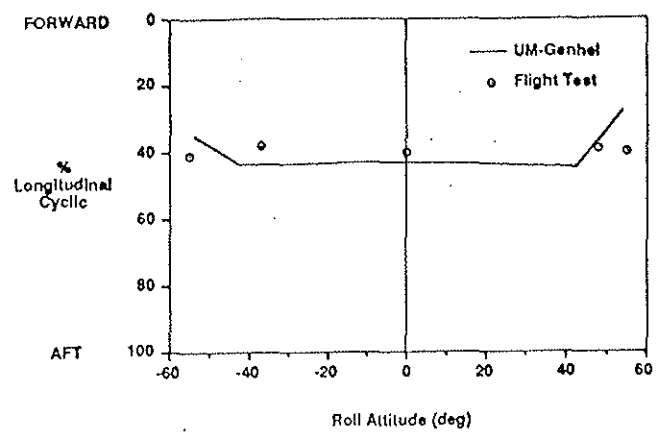
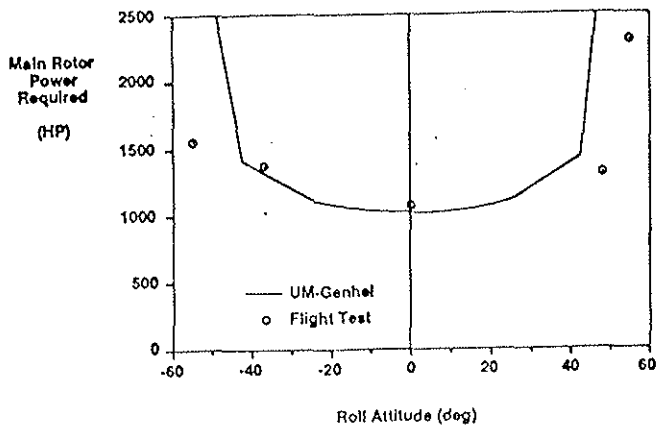


Figure 2: Trim state in coordinated steady level turn; V=100 kts.

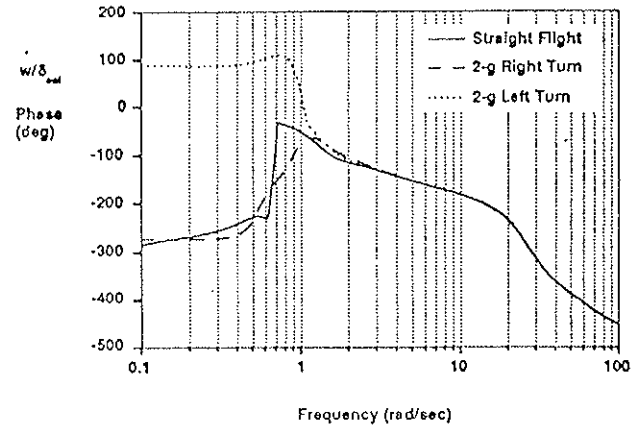
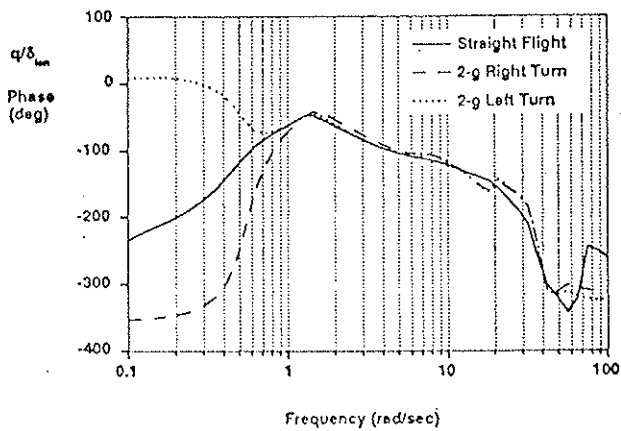
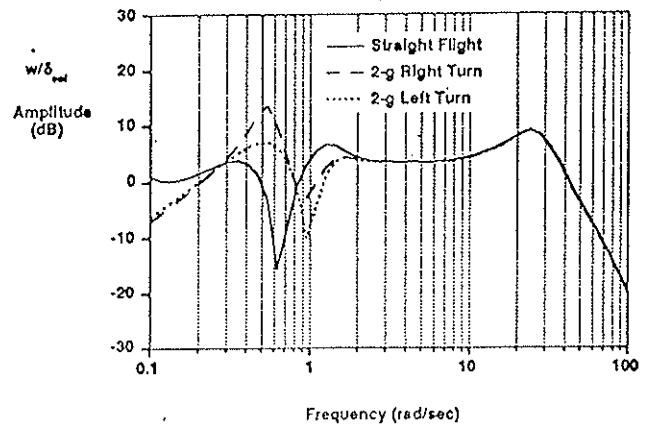
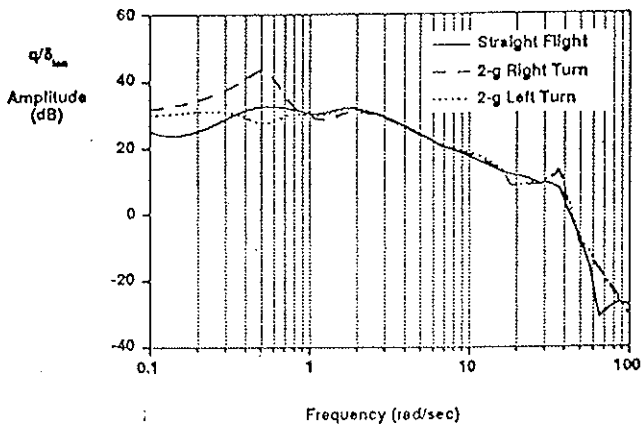
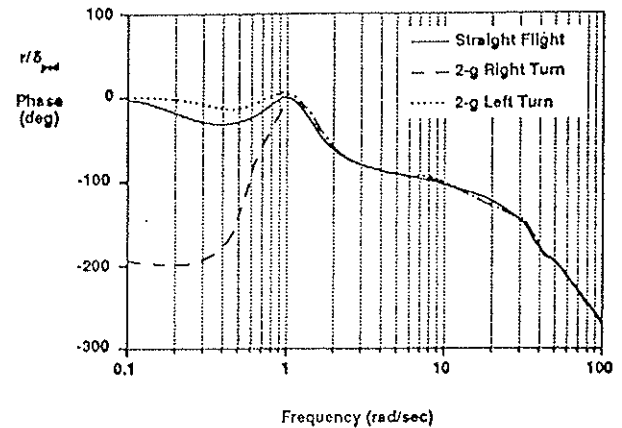
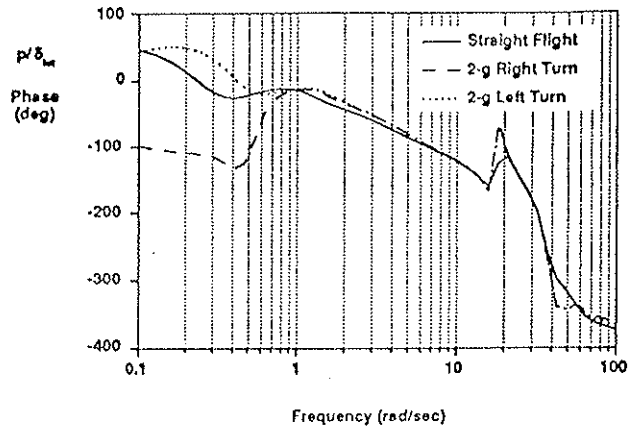
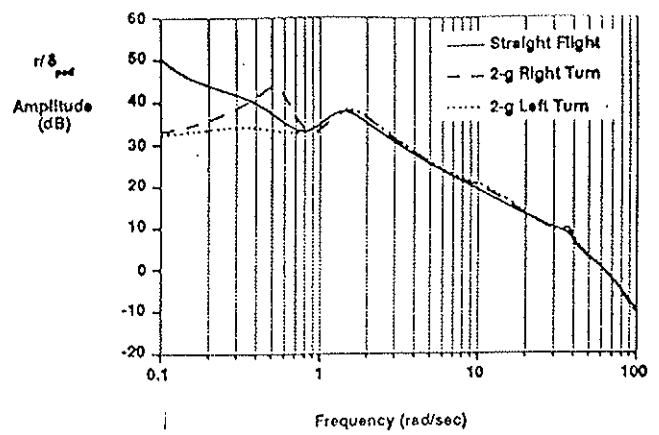
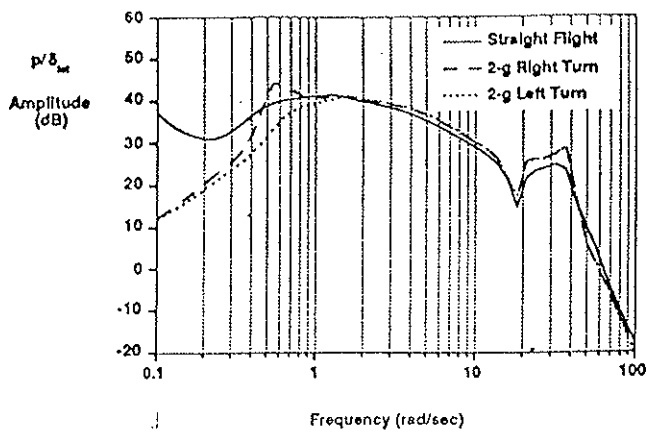


Figure 3: On-axis frequency response in right and left 2-g turns;  $V=80$  kts.

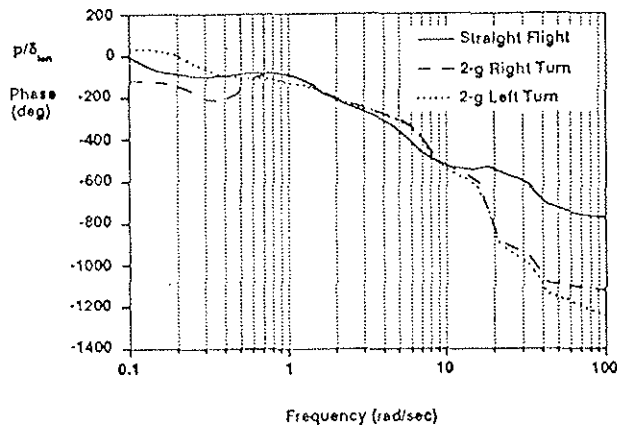
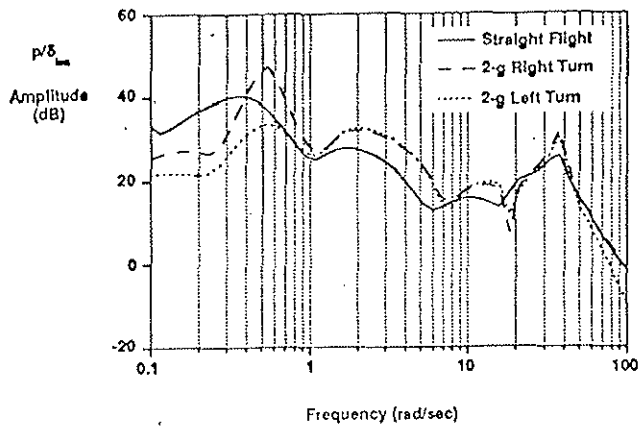
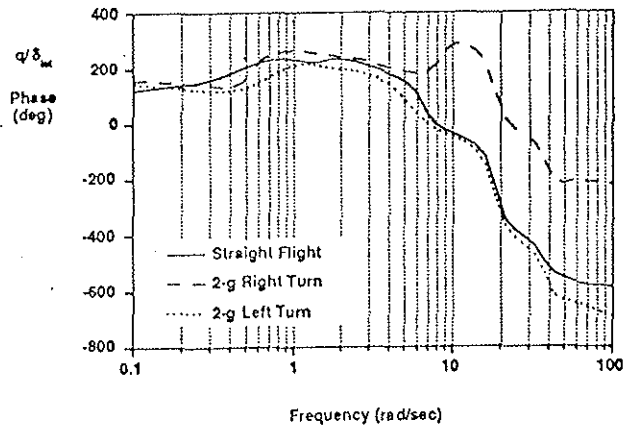
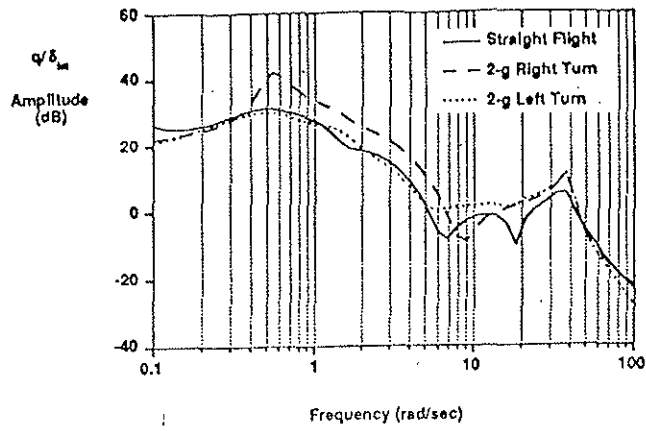


Figure 4: Off-axis frequency response in right and left 2-g turns;  $V=80$  kts.